



# Triple-fusion protein (TriFu): A potent, targeted, enzyme-like inhibitor of all three complement activation pathways

Received for publication, July 26, 2023, and in revised form, February 5, 2024. Published, Papers in Press, February 23, 2024.  
<https://doi.org/10.1016/j.jbc.2024.105784>

Sophia J. Sonnentag<sup>1</sup>, Arthur Dopler<sup>1</sup>, Katharina Kleiner<sup>1</sup>, Brijesh K. Garg<sup>2</sup>, Marco Mannes<sup>3</sup>, Nadja Späth<sup>1</sup>, Amira Akilah<sup>1</sup>, Britta Höchsmann<sup>4,5</sup>, Hubert Schrezenmeier<sup>4,5</sup>, Markus Anliker<sup>4,5</sup>, Ruby Boyanapalli<sup>6</sup>, Markus Huber-Lang<sup>3</sup>, and Christoph Q. Schmidt<sup>1,7,\*</sup>

From the <sup>1</sup>Institute of Experimental and Clinical Pharmacology, Toxicology and Pharmacology of Natural Products, University of Ulm Medical Centre, Ulm, Germany; <sup>2</sup>Eurofins Lancaster Laboratories PSS, Cambridge, USA; <sup>3</sup>Institute of Clinical and Experimental Trauma Immunology, University Hospital of Ulm, Ulm, Germany; <sup>4</sup>Institute of Transfusion Medicine, University of Ulm, Ulm, Germany; <sup>5</sup>Institute of Clinical Transfusion Medicine and Immunogenetics Ulm, German Red Cross Blood Transfusion Service, Baden-Württemberg-Hessen and University Hospital of Ulm, Ulm, Germany; <sup>6</sup>Takeda Pharmaceuticals, Cambridge, Massachusetts, USA; <sup>7</sup>Institute of Pharmacy, Biochemical Pharmacy Group, Martin Luther University Halle-Wittenberg, Halle, Germany

Reviewed by members of the JBC Editorial Board. Edited by Clare E. Bryant

The introduction of a therapeutic anti-C5 antibody into clinical practice in 2007 inspired a surge into the development of complement-targeted therapies. This has led to the recent approval of a C3 inhibitory peptide, an antibody directed against C1s and a full pipeline of several complement inhibitors in preclinical and clinical development. However, no inhibitor is available that efficiently inhibits all three complement initiation pathways and targets host cell surface markers as well as complement opsonins. To overcome this, we engineered a novel fusion protein combining selected domains of the three natural complement regulatory proteins decay accelerating factor, factor H and complement receptor 1. Such a triple fusion complement inhibitor (TriFu) was recombinantly expressed and purified alongside multiple variants and its building blocks. We analyzed these proteins for ligand binding affinity and decay acceleration activity by surface plasmon resonance. Additionally, we tested complement inhibition in several *in vitro/ex vivo* assays using standard classical and alternative pathway restricted hemolysis assays next to hemolysis assays with paroxysmal nocturnal hemoglobinuria erythrocytes. A novel *in vitro* model of the alternative pathway disease C3 glomerulopathy was established to evaluate the potential of the inhibitors to stop C3 deposition on endothelial cells. Next to the novel engineered triple fusion variants which inactivate complement convertases in an enzyme-like fashion, stoichiometric complement inhibitors targeting C3, C5, factor B, and factor D were tested as comparators. The triple fusion approach yielded a potent complement inhibitor that efficiently inhibits all three complement initiation pathways while targeting to surface markers.

With the approval of the C5-inhibitory monoclonal antibody eculizumab for the treatment of the rare disease

paroxysmal nocturnal hemoglobinuria (PNH) in 2007, the complement cascade became druggable (1). Since then, eculizumab has also been approved for the treatment of atypical hemolytic uremic syndrome, anti-acetylcholine receptor antibody positive generalized myasthenia gravis, and anti-aquaporin-4 antibody-positive neuromyelitis optica spectrum disorder (2–4).

In 2018, ravulizumab, a second generation version of eculizumab with improved pharmacokinetic properties, was approved by the Food and Drug Administration for treatment of PNH patients (5, 6).

Both monoclonal antibodies bind C5 in 1:2 or 1:1 complexes, depending on whether an excess amount of antibody over C5 is available (as is generally expected with monospecific therapeutic immunoglobulin G antibodies).

C5 bound by eculizumab or ravulizumab cannot be proteolytically activated into the anaphylatoxin C5a and the larger split product C5b, which initiates the assembly of the membrane attack complex (MAC) (7, 8).

A C3 inhibitory peptide of the compstatin family (with two compstatin molecules linked by a polyethylenglycol linker) is also approved for the treatment of PNH (9, 10). A single compstatin moiety binds C3 and C3b (alongside C3c) in a 1:1 stoichiometry and inhibits C3 activation by convertases (11). More proximal blockage of the complement cascade by compstatin has the advantage of stopping the deposition of C3b onto PNH erythrocytes, thereby preventing both intravascular and extravascular hemolysis (9). The latter mode of hemolysis is active in a substantial proportion of PNH patients treated with C5 inhibitors (12–14).

Contrary to expectations, different versions of stoichiometric inhibitors targeting C3 or C5 failed to completely block activation of the complement terminal pathway (TP) *in vitro* and *in vivo*. For C3 inhibitors, this phenomenon was observed only after strong activation of the classical/lectin pathway (CP/LP), whereas for C5 inhibitors, strong activation of any initiation pathway resulted in residual lytic complement activity.

\* For correspondence: Christoph Q. Schmidt, [christoph.schmidt@uni-ulm.de](mailto:christoph.schmidt@uni-ulm.de).

## Complete complement inhibition by enzyme-like fusion protein

For stoichiometric C5 inhibitors, the phenomenon of pharmacodynamic breakthrough was first observed in the clinic and was later mechanistically deciphered (15–19). It describes the effect that conformational (rather than convertase-driven) C5 activation can occur under conditions of very strong complement activation even though C5 is inhibited. Strong complement activation in clinical settings is often referred to as “complement amplifying conditions” (17–20). Infections, trauma, and surgery represent typical “complement amplifying conditions”. While C3 inhibition by compstatin peptides efficiently blocks the alternative pathway (AP), CP/LP-induced C3 activation is strongly but not entirely inhibited (19).

Moreover, it has been established *in vivo* and *in vitro* that C5 activation can occur even in complete absence of functional C3 (19, 21). This phenomenon is denominated “C3-bypass activation of C5” (19). Previously, several preclinical studies reported incomplete TP inhibition by C3 inhibiting peptides under experimental conditions of strong activation of the CP/LP pathway, consistent with the phenomenon of C3 bypass activation. While a marked decrease in TP activity was consistently noted in these reports, an excess of C3 inhibitory peptides (over C3) did not completely inhibit (MAC) formation (22–25). A recent publication reporting the use of a C3 peptide inhibitor to treat critically ill COVID-19 patients enrolled in a clinical trial strongly supports the notion that stoichiometric C3 inhibitors do not block CP/LP activation substantially. Irrespective of the good suppression of C3 proteolysis in patients treated with a C3 peptide inhibitor, sC5b-9 levels remained very high, indicating ongoing TP activation (26). Taken together, different clinically developed or therapeutically used anticomplement agents that target the complement cascade at the levels of C3 or C5 fail to completely inhibit TP activation when all three initiation pathways are activated.

Here, we describe the identification of a novel engineered complement regulatory protein, triple fusion complement inhibitor (TriFu) that efficiently inhibits all three complement activation pathways. This protein designed through rational engineering of three different complement regulators targets host cell surface markers, the late stage-complement opsonins (iC3b and C3dg) and inhibits complement convertases in an enzyme-like fashion and therefore, unlike other inhibitors, is not rapidly consumed by the formation of long-lived inhibitor:target protein complexes. The rationally engineered and selected functionalities of TriFu (and several variants thereof) were evaluated in different *in vitro/ex vivo* assays head-to-head to several clinically available or clinically investigated inhibitors (and/or surrogates thereof) and shown to exhibit superior inhibitory activity. TriFu has the unique ability to efficiently block all three complement activation pathways.

### Results

#### Design and expression of fusion proteins that inhibit all complement pathways

To obtain a targeted, enzyme-like inhibitor that efficiently blocks all three activation pathways of the complement

cascade, selected domains with specific functionalities of three naturally occurring convertase directed inhibitors were combined into a single fusion protein. The four complement control protein (CCP) domains of decay accelerating factor (DAF) (or CD55) were fused to a polyglycine linker that connects to the CCP domains 19 to 20 of factor H (FH). An additional polyglycine linker connects the C terminus of DAF-FH(19–20) to the CCP domains 15 to 17 of complement receptor 1 (CR1) (or CD35) (Fig. S1). The resulting triple fusion protein combines (i) decay accelerating functionality toward all complement convertases with, (ii) cofactor activity (CA) for factor I mediated inactivation of C3b and C4b, and (iii) a targeting strategy recognizing the host surface markers sialic acids and glycosaminoglycans as well as the late stage opsonins iC3b and C3dg. Individual regulatory building blocks of TriFu, *i.e.* the CCP domain stretches of DAF and CR1 were produced for comparative purposes. In addition, intermediate fusion versions comprising the first two building blocks DAF and FH (19–20) were produced to compare the functionalities of the fusion strategy. Selected sequence variations were introduced into TriFu or single building blocks to tweak their regulatory activities toward one pathway or to increase the overall inhibitory activity. Published data were used to guide the selection of these variations which included the deletion of a selected domain, single or combined point mutations (which are listed in Fig. S2) (27–31). In addition, the length of the first polyglycine linker connecting different CCP domain stretches was varied. Linker lengths were modified to allow or prohibit simultaneous occupation of the two C3b binding domain stretches within the corresponding fusion proteins, *i.e.* DAF(1–4) and FH (19–20) (32, 33) (Fig. S3). The different building blocks and fusion protein variants were expressed into the culture medium (without tags) using the heterologous host *Pichia pastoris* (which has been reassigned into the “*Komagataella*” genus). All proteins were purified from the supernatant by typically combining three consecutive protein chromatography steps as described in methods (in analogy to previously established purification protocols (34, 35)). A high purity for all the protein constructs was reached (Fig. S4).

#### Binding of protein building blocks and engineered fusion proteins to C3b and C4b is retained

A prerequisite for convertase directed regulation *via* cofactor and/or decay accelerating activity (DAA) is the ability to bind to the complement proteins C3b and C4b (Fig. S1) (36). First, the affinities for C3b were determined by surface plasmon resonance (SPR) (Fig. S5A). The parts of the natural regulators that comprise the building blocks of TriFu, *i.e.* the first four CCP domains of DAF, DAF(1–4), the two C-terminal domains of FH, FH(19–20), and the middle domains of CR1, CR1(15–17), exhibited affinities for C3b of 11  $\mu$ M, 4.7  $\mu$ M, and 0.9  $\mu$ M, respectively. This is in line with previously reported affinities for C3b by these recombinant proteins (32, 35, 37–40). Next, the intermediate fusion version, *i.e.* the fusion between DAF(1–4) and FH(19–20) was investigated. Two different variants of this fusion were prepared. One with a

polyglycine linker of 13 residues, denominated DAF(1–4)FH(19–20)-LL (where LL stands for long linker). Thirteen glycine residues can span a distance of  $13 \times 3.8 \text{ \AA} (= 49.4 \text{ \AA})$ . This linker is expected to easily bridge the necessary distance of  $32 \text{ \AA}$  allowing both C3b-binding patches within DAF(1–4)FH(19–20)-LL to engage C3b simultaneously (Fig. S3). The variant with a short linker (SL) is denominated DAF(1–4)FH(19–20)-SL. It contains only a “GPGG” peptide stretch to link the DAF(1–4) to the FH(19–20) polypeptide stretch. For this variant a simultaneous occupation of both binding patches on one C3b molecule is not possible. The linker length of the double fusion protein DAF(1–4)-FH(19–20) did indeed impact on the affinity for C3b immobilized on an SPR chip surface. The variant with the SL exhibited visibly slower association and dissociation phases. The apparent affinity, as measured by the equilibrium dissociation constants ( $K_D$ ), was slightly higher for the SL fusion protein. DAF(1–4)FH(19–20)-SL and -LL exhibited affinities of 125 and 175 nM, respectively (Fig. S5A). Next, different linker versions of the triple fusion were tested for C3b binding. The linker between the DAF and the FH CCPs (*i.e.*, the first linker) was varied. TriFu\_no\_linker did not contain any polyglycine linker. The connection between the last conserved cysteine of DAF CCP 4 and the first conserved cysteine of FH CCP 19 (including the cysteines) is “CRGGKC”. Up to two amino acids before the first or after the last conserved cysteine of a CCP module are part of the actual CCP domain. The two glycines in the “CRGGKC”-stretch are the last and first natural amino acid sequence of DAF CCP 4 and FH CCP 19, respectively. For the construct TriFu\_6G and TriFu\_13G either 6 or 13 glycine residues, respectively, were inserted as polyglycine linker residues. Only the 13 glycine linker variant is expected to allow for simultaneous occupation of the DAF(1–4) and FH(19–20) binding patches on one C3b molecule (Fig. S3). Full-length FH was also assayed as a reference. FH is known to contain two C3b binding patches, one at each of its termini. FH was found to exhibit a  $K_D$  of 802 nM, in line with published reports (32, 35) (Fig. S5B). All TriFu linker variants contain three C3b binding stretches located within the CCP stretches of DAF(2–4), FH(19–20), and CR1(15–17). The patches of DAF(2–4) and CR1(15–17) have mostly overlapping binding sites on C3b, while FH(19–20) binds to another site on C3b (*i.e.* the thioester domain that corresponds to C3d). With apparent affinities for the C3b sensor chip surface (at a C3b loading of 300 response units) of 98, 59, and 25 nM for the TriFu versions “no-linker”, “6G” and “13G”, respectively, an 8-, 14- and 32-fold increase in affinity for C3b was achieved for the triple fusion proteins when compared to FH. While the C3b affinity for the “13G” variant was about twice as high as for the “6G” variant, the dissociation phase of the latter was visibly slower than the ones for the “13G” and the “no-linker” (without; wo) variant. This indicates that the spacing and flexibility between DAF(1–4) and FH(19–20) have an impact on the time that the TriFu variants remain associated with a C3b-loaded surface. TriFu\_6G was investigated further for C3b and C4b binding (using a higher C3b density on the SPR chip compared to above). The affinity of 50 nM for C3b binding is consistent

with the results on the lower density C3b surface (above) (Fig. 1). C4b binding by TriFu\_6G has an apparent estimated  $K_D$  of 865 nM and thus is about 17-fold weaker than the affinity for C3b binding. TriFu\_6G contains two binding stretches for C4b (*i.e.* DAF(1–4) and CR1(15–17)), while all three functional units of TriFu bind to C3b. DAF(1–4) and CR1(15–17) were also tested for C4b binding. This time, C4b was captured *via* its thioester moiety in physiological orientation (instead of random orientation achieved by amine coupling) (Fig. S6, A–C). DAF(1–4) and CR1(15–17) exhibited apparent  $K_D$  values of 17.6  $\mu\text{M}$  and 7.8  $\mu\text{M}$ , respectively. TriFu\_6G has an affinity of 643 nM on this sensor chip surface immobilized with physiologically oriented C4b. When both C4b binding sites are connected (as within TriFu\_6G), avidity for the binding to a C4b deposited surface is induced, as expected. The binding of TriFu to the late stage opsonins iC3b and C3d (coupled *via* standard amine coupling) was also analyzed by SPR. TriFu\_6G exhibits an estimated binding affinity of about 22  $\mu\text{M}$  for the C3d sensor chip. The interaction is about fourfold weaker than the reported affinity of FH(19–20) binding to C3d of 4 to 6  $\mu\text{M}$  (32, 38). This is likely due to the embedding of FH(19–20) between DAF(1–4) and CR1(15–17) within the context of TriFu. It was reported that the addition of CCP 18 to FH(19–20) weakened the binding activity of FH(19–20) for C3d yielding an affinity of about 10  $\mu\text{M}$  for the construct FH(18–20) (38).

### Complement inhibition activity of protein building blocks and engineered fusion proteins

In addition, and similar to the C3b and C4b binding analysis, the complement inhibitory activity was first tested for the TriFu building blocks and the 13G linker variant of TriFu. A standard rabbit hemolysis assay in 25% serum demonstrates that the triple fusion variant is the most active inhibitor compared to the TriFu building blocks (Fig. S7A). Remarkably, the double fusion protein with a long glycine linker sequence of 13 glycines, DAF(1–4)FH(19–20)-LL, is substantially more active than DAF(1–4)FH(19–20)-SL which has only the four “natural” linking residues “GPGG”. The building block of CR1(15–17), which only has CA, appears to be slightly more active in preventing hemolysis than the building block of DAF(1–4), which only has decay accelerating activity and shows the lowest inhibitory activity in this assay.

In an AP restricted hemolysis assay with PNH-erythrocytes at a final serum percentage of 75%, TriFu\_13G ( $IC_{50} = 0.09 \mu\text{M}$ ;  $R^2 = 0.91$ ) was about twofold more active than (soluble complement receptor 1 [sCR1] ( $IC_{50} = 0.18 \mu\text{M}$ ;  $R^2 = 0.85$ )) (Fig. S7B). The linker length of the building block DAF(1–4)FH(19–20) had no influence on the activity. The single building blocks DAF(1–4) and CR1(15–17) were the least active. A typical CP-mediated hemolysis assay in 5% and 75% final serum content revealed that the triple fusion protein TriFu inhibited the CP more actively than any of the building blocks (Fig. S7, C and D). In addition, TriFu\_13G ( $IC_{50} = 0.10 \mu\text{M}$ ;  $R^2 = 0.98$ ) was approximately twofold more active than sCR1 ( $IC_{50} = 0.24 \mu\text{M}$ ;  $R^2 = 0.97$ ) in protecting sensitized

## Complete complement inhibition by enzyme-like fusion protein

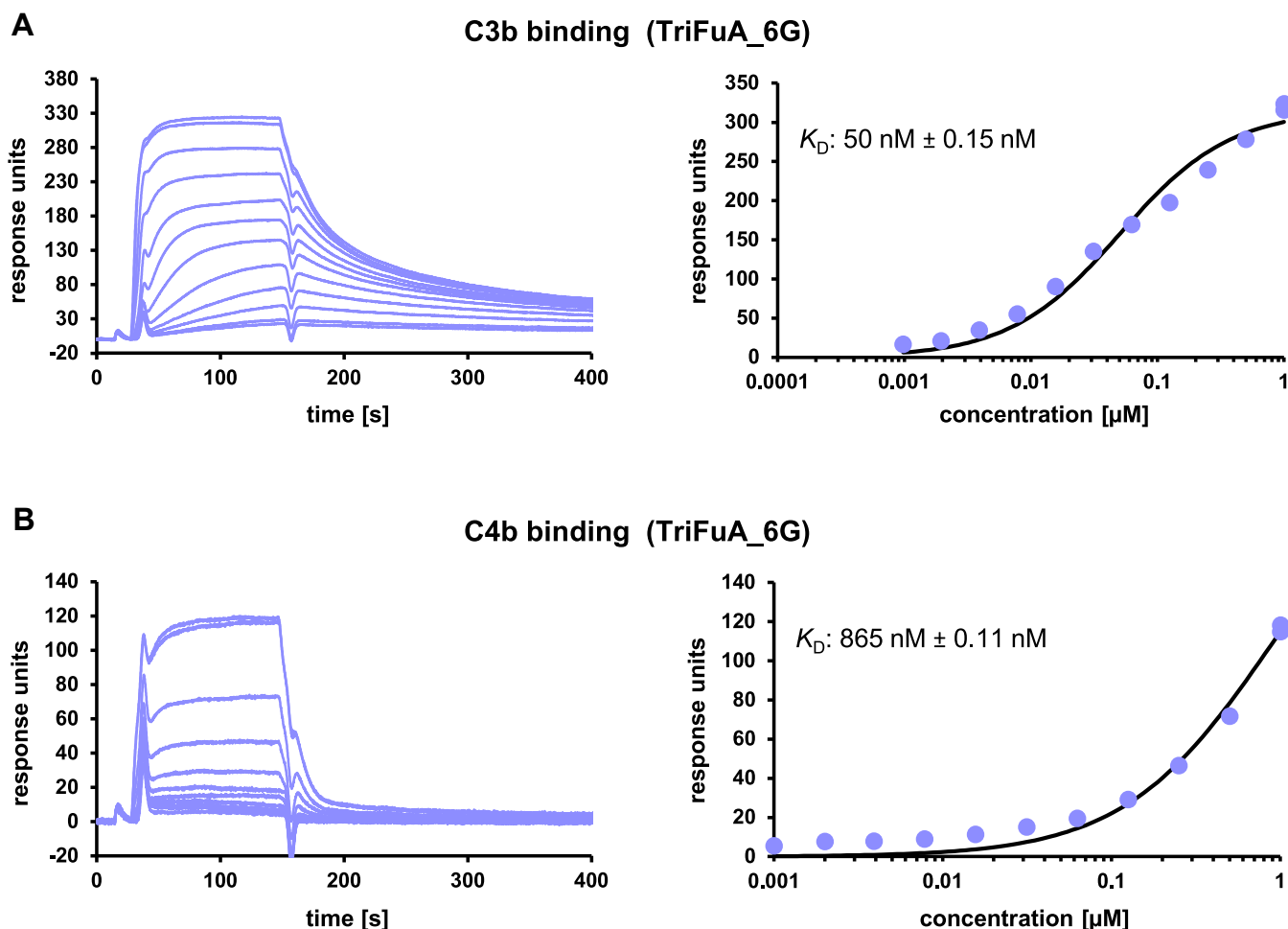


**Figure 1. C3b and C4b binding affinity of TriFu\_6G.** A, TriFu\_6G was applied onto a carboxymethyl dextran sensor chip surface (CMD500m from Xantec Bioanalytics) on a Reichert SR7500DC SPR instrument at 25 °C with 2070 RU of C3b immobilized *via* standard amine coupling. The *left* display shows the sensorgrams of the concentration series. The *right* display shows the corresponding response *versus* concentration plot and the 1:1 affinity fit. B, as in (A) but TriFu\_6G was assayed for C4b binding with 4820 RUs of C4b being immobilized *via* amine coupling onto a carboxymethyl dextran sensor chip surface (CMD500m from Xantec Bioanalytics) measured on a Reichert SR7500DC SPR instrument at 25 °C. CMD, carboxymethyl dextran; RU, relative unit; SPR, surface plasmon resonance; TriFu, triple fusion complement inhibitor.

sheep erythrocytes from complement-mediated lysis. It is noteworthy that although the individual building blocks DAF(1–4) and CR1(15–17) had approximately the same equal inhibitory effect toward the AP, the latter was a much weaker inhibitor toward the CP at a low serum levels. Additionally, both individual building blocks failed to completely inhibit complement-mediated hemolysis after CP activation in a serum content of 75%. Even inhibitor concentrations of 100 to 200  $\mu\text{M}$  were not sufficient to completely protect the sensitized red blood cells.

### Hemolysis assays to assess the inhibitory potential of engineered convertase-directed inhibitors and stoichiometric inhibitors

Since different linker length between the first two building blocks of TriFu, *i.e.* DAF(1–4) and FH(19–20) had some influence on C3b binding activity (Fig. S5), three TriFu variants with different linker lengths (at their first molecular junction) were investigated for their inhibitory activity in a standard

complement-mediated hemolysis assay. Within the triple fusion proteins, the linker length did not impact on the activity to inhibit AP-mediated hemolysis (Fig. 2A). This contrasts with the different linker lengths of the double fusion proteins containing only the first two building blocks (Fig. S7B). The addition of the third building block appeared to largely annihilate any differences that were caused by the linker length within the double fusion proteins. Therefore, in further assays either the 6G or the 13G version of TriFu was used as functionally equivalent variants. Another standard AP-mediated hemolysis assays in 25% serum content was used to compare the activity of TriFu to stoichiometric inhibitors and miniFH (Figs. 2B and S9A). TriFu was fivefold to tenfold more active than the engineered and AP specific miniFH molecule. TriFu also outperformed the anti-C5 approach which has a visibly higher  $\text{IC}_{50}$  and, importantly, suffers from substantial residual C5 activity (consistent with previous publications (17–19)). As expected, the anti-factor D (anti-FD) approach was the most active considering the low serum concentration of FD. In an additional AP hemolysis assay using a higher serum content of

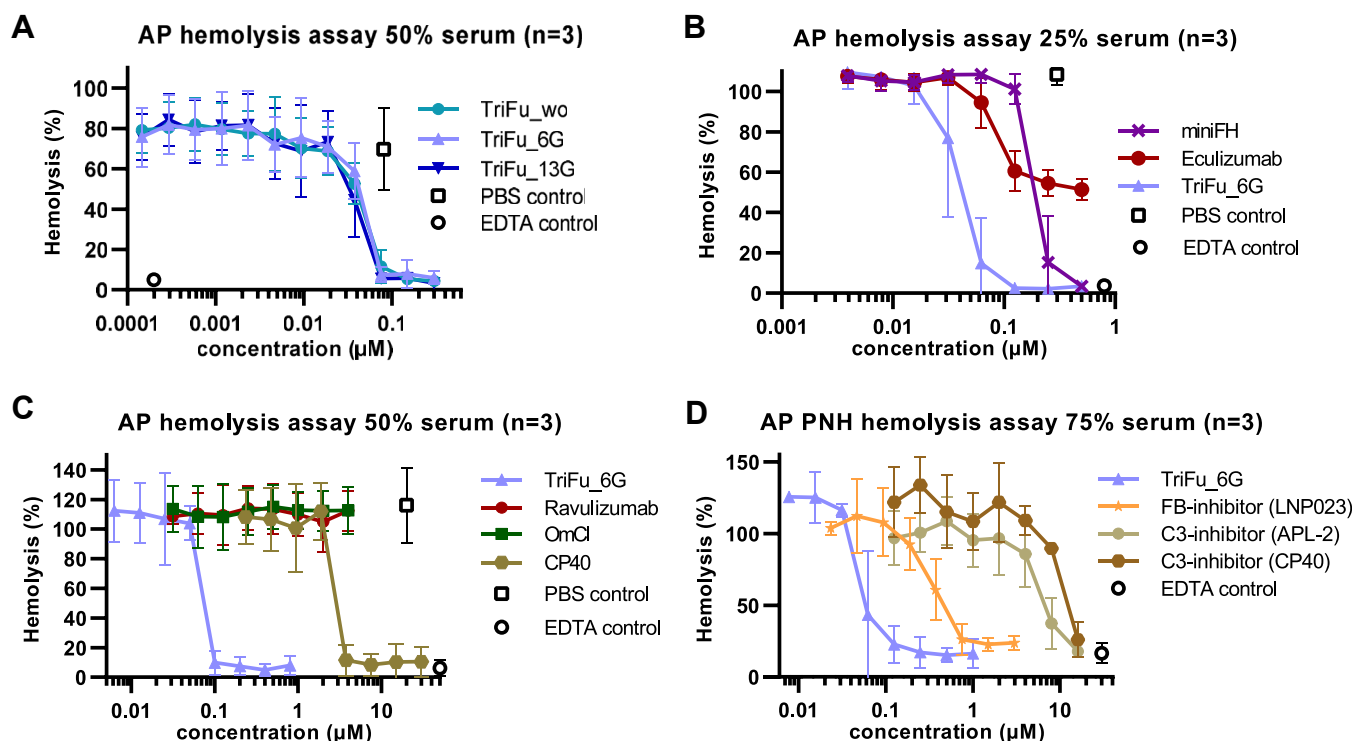


**Figure 2. Inhibition of AP-mediated hemolysis by TriFu variants and comparison to stoichiometric complement inhibitors.** A, TriFu versions with three different linker length were tested in a standard AP-mediated hemolysis assay using rabbit erythrocytes in a final serum content of 50% serum. Lysis in H<sub>2</sub>O served as a control for 100% lysis and was used to normalize the data. Mean values of three independent assays with standard deviation are shown. B, TriFu<sub>6G</sub> was compared to miniFH and eculizumab. Same assay as in (A). Mean values of three independent assays with standard deviation are shown. C, standard AP-mediated hemolysis assay in a higher serum content of 50% comparing the activity of TriFu<sub>6G</sub> to ravulizumab OmCI and CP40. Mean values of three independent assays with standard deviation are shown. D, PNH hemolysis assay with a final serum content of 75%. Serum (from different donors of unknown blood group) was slightly acidified (as described in methods according to the modified Ham's test) and mixed with Mg-EGTA prior to supplementation with analytes and PNH erythrocytes. Level of lysis was normalized to lysis that was observed when PBS instead of a complement inhibitor had been added to the acidified serum. Mean values of three independent assays with standard deviation are shown. AP, alternative pathway; FH, factor H; OmCI, *Ornithodoros moubata* complement inhibitor; PNH, paroxysmal nocturnal hemoglobinuria; TriFu, triple fusion complement inhibitor.

50%, TriFu was compared to ravulizumab, *Ornithodoros moubata* complement inhibitor (OmCI), the tick-derived C5 inhibitor in clinical development (also known as coversin which binds C5 in a 1:1 complex) and the C3 inhibitory cyclic peptide CP40 which is also developed clinically (Figs. 2C and S9B). Increasing the serum content in the assay from 25% to 50% made it necessary to increase the TriFu concentrations to achieve complete inhibition of hemolysis. The higher serum content dramatically increased the residual, lytic C5 activity of the C5 inhibitors from about 40% or 50% (in 25% serum) to about 70% or 100% (in 50% serum) (Figs. 2, B and C and S9, A and B). This demonstrated that C5 inhibition is indirectly proportional to the strength of the complement activation as previously established (18). Once the CP40 concentration reached the C3 level in the assay, AP-mediated hemolysis was completely inhibited. The AP inhibitory activity of TriFu was also assessed in a clinically meaningful AP assay analyzing the lysis of patient derived PNH erythrocytes in a modified Ham's test. TriFu was about fivefold more efficient in preventing hemolysis of PNH erythrocytes in comparison to a surrogate of the factor B (FB) inhibitor LNP023 (Fig. 2D). The two different C3 inhibitors peptides protected the PNH erythrocytes as soon as all C3 molecules were occupied by the respective inhibitor in the assay. As the surrogate of the C3 inhibitory peptide

APL-2 contains two compstatin rings in one molecule linked by PEG chains, it was about twice as active as CP40 which comprises one compstatin ring.

Next, CP activities were assessed. Evaluating the three TriFu versions with different linker length in a CP assay (of 50% serum content) demonstrated overall similar regulatory activities of the different fusion approaches (Fig. 3A). Using the same assay setup, the activity of TriFu was compared to miniFH and several stoichiometric inhibitors. As expected, miniFH, being AP specific, did not show inhibitory activity in this CP assay (Figs. 3B and S10, A and B). Eculizumab, ravulizumab, OmCI, and a PASylated version of OmCI (PAS-OmCI) protected the sensitized sheep erythrocytes from hemolysis. Eculizumab and ravulizumab were about twofold more effective than OmCI/PAS-OmCI consistent with their 1:2 and 1:1 binding stoichiometry to C5, respectively. The compstatin version CP40 assayed at 10  $\mu$ M showed no or only a minor protection from CP-mediated hemolysis at a serum content of 50%. This is remarkable since 4  $\mu$ M of CP40 almost completely protected from AP-mediated hemolysis at an equal serum content of 50% (compare Figs. 2C and 3B). That inhibition of C3 by stoichiometric inhibitors (or absence of C3) does not protect from CP mediated lysis has been established before,

## Complete complement inhibition by enzyme-like fusion protein

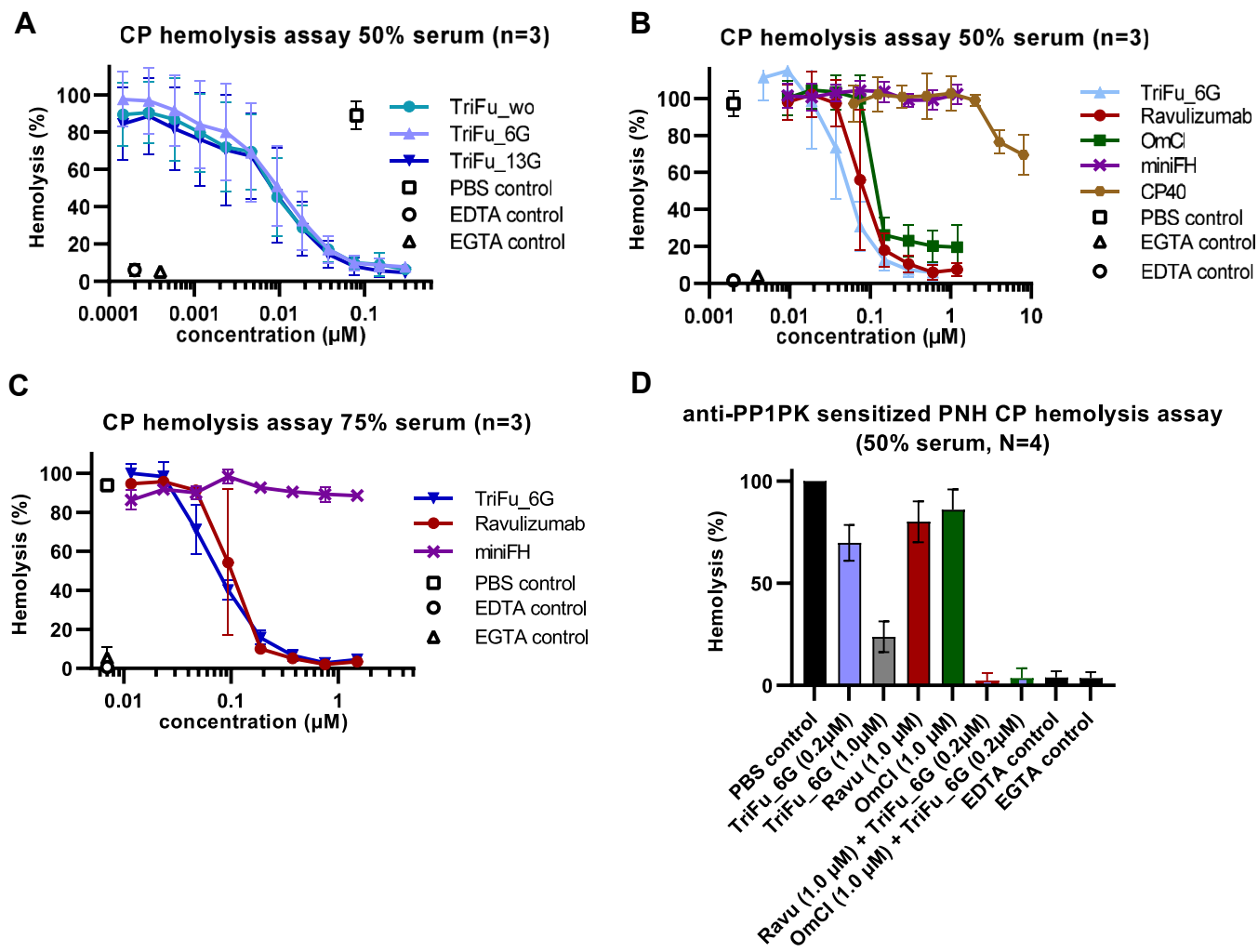


**Figure 3. Inhibition of CP-mediated hemolysis by TriFu variants and comparison to stoichiometric inhibitors.** A, three different TriFu version with three different linker length were tested in a CP-mediated hemolysis assay using sensitized sheep erythrocytes in (a higher than normal) final serum content of 50% serum. Lysis in H<sub>2</sub>O served as a control for 100% lysis and was used to normalize the data. Mean values of three independent assays with standard deviation are shown. B, the inhibitory activity of TriFu\_6G toward the CP was compared to ravulizumab, OmCI, miniFH, and CP40. Same assay as in (A). Mean values of three independent assays with standard deviation are shown. C, CP-mediated hemolysis assay in a higher serum content of 75% was used to compare the activity of TriFu\_6G to miniFH, and ravulizumab. Mean values of three independent assays with standard deviation are shown. D, CP initiated PNH hemolysis assay without serum acidification at a final serum content of 50%. The alloantibody PP1Pk was used to further sensitize the already vulnerable PNH erythrocytes from PNH patients prior to exposing them to complement active serum that had been supplemented with analytes or controls as indicated. The level of lysis was normalized to lysis observed when PBS instead of a complement inhibitor had been added. Mean values of four independent assays with standard deviation are shown. Fig. S8 shows representative flow cytometry data analyzing the type of PNH erythrocytes that survived the assay conditions. CP, classical pathway; FH, factor H; OmCI, *Ornithodoros moubata* complement inhibitor; PNH, paroxysmal nocturnal hemoglobinuria; TriFu, triple fusion complement inhibitor.

illustrating the C3-bypass activation route of C5 (19, 21). Another CP hemolysis assay was performed at a final serum content of 75%. This demonstrated that TriFu efficiently blocks CP-mediated lysis also at higher serum percentages (Fig. 3C). As expected, AP selective inhibitors did not show inhibitory potential in this setup. Finally, TriFu, selected C5 inhibitors and combinations of TriFu and C5 inhibitors were tested in a very sensitive CP-mediated hemolysis assay using alloantibody sensitized PNH erythrocytes. While TriFu at 1  $\mu$ M reduced hemolysis by about 80%, the same concentration of either ravulizumab or OmCI only reduced hemolysis by about 20% (Fig. 3D). At a concentration of 0.2  $\mu$ M, TriFu was as active as the C5 inhibitors at 1  $\mu$ M. Note that the C5 concentration in 50% serum is only about

0.25  $\mu$ M. A combination of 1  $\mu$ M of a C5 inhibitor together with 0.2  $\mu$ M of TriFu could completely inhibit hemolysis.

### Attempt to further increase overall inhibitory activity, and to introduce complement pathway selectivity of TriFu

TriFu was conceptualized to be a potent inhibitor that efficiently regulates all the complement activation pathways by combining selected domains of three different complement regulators. Published data are available describing point mutations and domain deletion versions of the building blocks of TriFu that increase or decrease DAA or CA for one or all proximal complement pathways. We produced TriFu versions that contained domain deletions or selected point mutations

or combinations thereof to either increase or decrease the activity of TriFu for one pathway. The rationale behind these sequence variations and a table summarizing the functional outcome is presented in Fig. S2. Introduction of amino acid substitution reported to boost the DAA of DAF(1–4) had little overall effect within the TriFu fusion protein. The reason for this could be that the activity of TriFu is already much stronger than that of DAF(1–4), which does not lead to any further increase in activity when point mutations are introduced into the first building block of TriFu. The attempts to achieve relative pathway selectivity were more successful as the inhibitory activity could be tweaked toward favoring AP inhibition: e.g., TriFu\_V7 was as active toward the AP as the WT TriFu version, but it was substantially less active in inhibiting the CP. This resulted in a 10-fold selectivity for inhibiting the AP. In addition to introducing sequence variations within the TriFu protein scaffold, three sequence variants of the CR1(15–17) building block were also investigated for their effect on CA. However, the mutant versions S1089R and D1076R had no impact on the CA of CR1(15–17), while the version D1009R lost all its activity for both, AP and CP-specific CA (Fig. S11). Thus, the investigated sequence changes in CR1(15–17) were not helpful in potentiating the overall activity or tweaking the pathway specificity. Yet, these data may be useful for future research efforts that further characterize the natural complement regulators DAF and CR1.

**Assessment of TriFu and stoichiometric inhibitors in protecting endothelial cells from complement attack**

An *in vitro* model of C3 glomerulopathy was established by exposing cultured human microvascular endothelial cells (HMEC-1) to FH-depleted serum and the level of C3 deposition on the endothelial cell surfaces were measured. It is expected that complement activation in FH-depleted serum is initiated through the AP, and thus EGTA was not supplemented initially. The inhibitory activities of TriFu, miniFH, and FH were compared to each other. All three inhibitors showed a clear protection from C3 deposition at higher inhibitor concentrations. Remarkably, TriFu appeared to be somewhat more

effective as it inhibited the C3 deposition to a higher extent than FH and miniFH (Figs. 4A and S12). We speculated that potentially some levels of CP/LP activity may be present in the assay conditions on the tissue culture plates coated with HMEC-1 cells. This could potentially explain why the AP specific inhibitors FH and miniFH were not completely effective. Therefore, in a second assay, we compared the activities of TriFu to an AP-selective FB inhibitor and a peptide inhibitor of C3 and included EGTA in the assay conditions to specifically exclude CP/LP activity. TriFu was the most potent inhibitor efficiently preventing C3 opsonization on the endothelial cells at a concentration of 0.25 μM and higher (Figs. 4B and S12). The C3 inhibitor also efficiently prevented C3-deposition at concentrations that were higher than the C3 concentration in the assay. Although the surrogate of the FB inhibitor LNP023 substantially limited C3 deposition on endothelial cells, it could not completely inhibit it at concentrations up to 8 μM.

**Serum bactericidal activity in presence of different complement inhibitors**

Gram-negative bacteria are known to be especially sensitive to MAC-mediated cytotoxicity. To rule out substantial interference with bacterial killing, the effects on serum bactericidal activity of TriFu, a stoichiometric C5 inhibitor (an eculizumab surrogate molecule) and a stoichiometric C3 inhibitor (an APL-2 surrogate molecule) were investigated in an *in vitro* system. Therefore, *Escherichia coli* cells were exposed to serum that had been supplemented with selected complement inhibitors. Two TriFu variants and the eculizumab surrogate were assayed at concentrations of 0.2 and 0.4 μM, corresponding to the concentrations that provided protection from AP- and CP-mediated hemolysis (in assays also containing a final serum percentage of 50%, see Figs. 2C and 3B). These concentrations influenced bactericidal serum killing of *E. coli* to a clear but minor extent (Fig. 5). Stoichiometric FB and C3 inhibitors were assayed in the bactericidal assay at 1 μM and 10 μM, respectively. These concentrations provided a good protection against AP-mediated hemolysis (Fig. 2) but had no effect on the serum bactericidal activity that eliminates *E. coli* cells (Fig. 5). It is already known

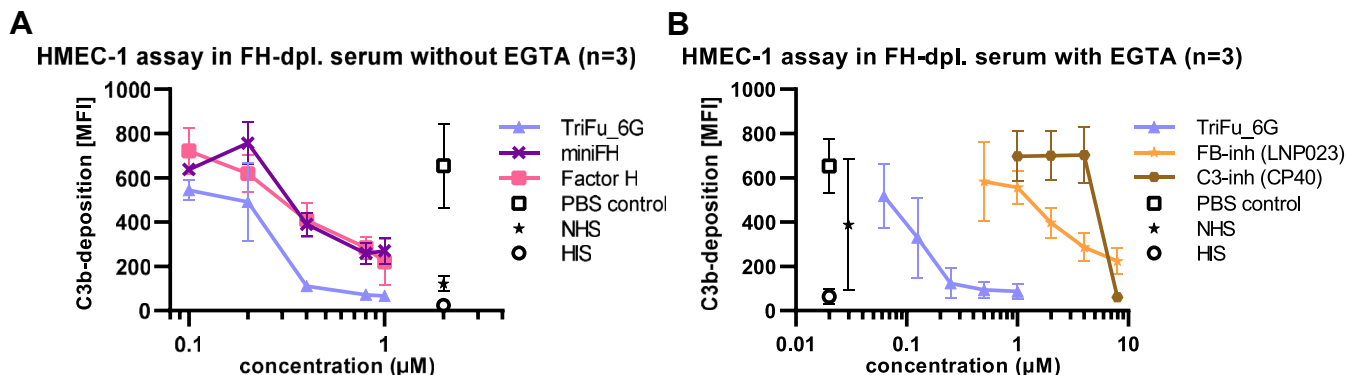


**Figure 4. Protection of human endothelial cells from C3 opsonization in an *in vitro* model of C3 glomerulopathy.** Endothelial cells (HMEC-1) were incubated with NHS, HIS, or FH-depleted serum that had been supplemented with analytes as indicated. The final serum content in the assay was 40%. After incubation at 37 °C for 1 h, the supernatant was discarded, and the cells were harvested and analyzed for C3b deposition by flow cytometry using a monoclonal anti-C3d antibody. Mean values of the measured median fluorescent intensity (MFI) of three independent assays with SD are shown. A and B, show data with and without supplementation of EGTA in the assay, respectively. Representative histograms of the flow cytometry data are shown in Fig. S12. FH, factor H; HIS, heat-inactivated serum; HMEC, human microvascular endothelial cells; NHS, normal human serum.

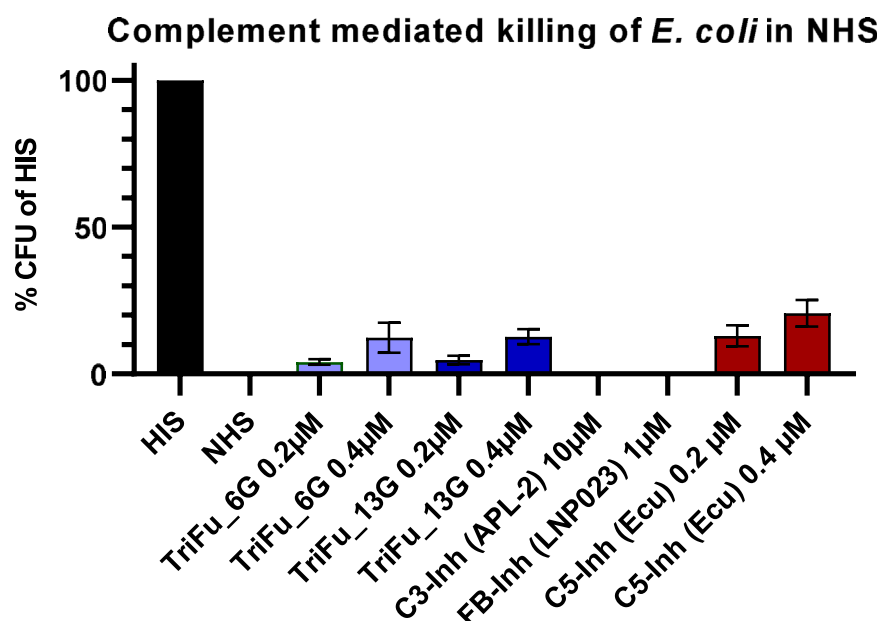


**Figure 5. Complement mediated killing of *Escherichia coli* in NHS.** *E. coli* cells containing a selective marker were incubated for 1 h in NHS supplemented with complement inhibitors or PBS. The final serum content in the assay was 50%. Colony forming units (CFU) were evaluated by colony counting after plating the reactions on selective medium. The resultant CFU were normalized to the CFU obtained when heat inactivated serum (HIS) was used instead of NHS. Mean values of three technical replicates with standard deviation are shown. NHS, normal human serum.

that inhibition of the AP by FD or FB inhibitors does not to substantially affect bactericidal activity in the serum of donors vaccinated against the relevant bacteria (41, 42). Consistent with this notion, published data show that antibody-dependent and independent CP activation leads to complement-mediated lysis of *E. coli* even if the AP is blocked (43, 44). Since C3-bypass activation of C5 has been previously reported (19, 21) and is also shown here in presence of stoichiometric C3 inhibitors (Fig. 3B), it is expected that CP-mediated cytolysis occurs under C3 inhibition (as shown *e.g.* for foreign *E. coli* or host-like antibody sensitized erythrocytes).

## Discussion

Several fusion proteins were engineered to contain selected domains of natural convertase directed complement inhibitors. The aim was to construct efficient complement inhibitors that prevent breakthrough lysis for potential clinical use that utilize the functionality of natural complement regulators. To arrive at a high regulatory potency at much lower doses, the selected functions of the three complement regulators DAF, FH, and CR1 were combined into one fusion protein approach denominated TriFu. Different lengths of glycine linkers that connect the domain stretches of the three natural regulators were evaluated. These trimolecular fusion proteins and their building blocks were systematically analyzed for structure activity relationships and their complement regulatory activities were compared *in vitro* with those of several stoichiometric inhibitors in clinical use and/or clinical development.

The analysis of different linker lengths connecting the first building block DAF(1–4) to FH(19–20) demonstrated higher AP regulatory activity of the LL version, which allows simultaneous engagement of the DAF and FH(19–20) binding sites

on C3b. However, this higher efficiency of the longer linker variant was lost when the double fusion construct was extended by CR1(15–17). The most likely explanation for this observation is that the addition of CR1(15–17) to the double fusion of DAF(1–4)-FH(19–20) (containing either SLs or LLs) boosts the overall activity to such an extent that the differences in activity introduced by the different linker lengths within the double fusion constructs were annihilated.

The complement regulatory activity of the single building blocks DAF(1–4) and CR1(15–17) was also assessed and compared to the activities of the fusion protein versions. This comparison showed that the single building blocks containing either only DAA or CA, respectively, exhibited substantial AP and CP regulatory activity in serum assays that contain relatively low serum percentages. Under these conditions either DAA or CA is sufficient for efficient protection of erythrocytes from AP- or CP-mediated lysis. However, in higher serum percentages, when the amplification loop of the AP comes into action, each regulator with a single functionality (of DAA or CA) has very limited regulatory activity compared to the fusion molecules that contain both complement regulatory functions simultaneously. Even inhibitor concentrations of 100 to 200 µM did not suffice to completely protect the sensitized red blood cells (Fig. S7, C and D). Therefore, to efficiently disrupt the AP amplification loop, both the C3 convertase C3bBb as well as C3b, which serves as platform to assemble new convertases, must be regulated to achieve an efficient regulatory response in assays of higher serum content.

Engineered convertase-directed regulators exhibiting a natural regulatory mode were hypothesized to overcome the issues observed for the clinically used stoichiometric inhibitors of C3 and C5. These are unable to completely inhibit the lytic TP after strong activation of the CP/LP or any pathway, respectively



(reviewed in (45)). To prove our hypothesis, the complement regulatory activity of the engineered TriFu protein was compared to the activities of stoichiometric complement inhibitors targeting C3 (CP40 or an APL-2 surrogate), C5 (eculizumab, ravulizumab, an eculizumab surrogate or OmCI), FB (an LNP023 surrogate) or FD. In each *in vitro* assay, TriFu was able to completely inhibit TP activation or C3b-deposition, while all stoichiometric inhibitors tested, except the anti-FD antibody, failed to do so. The latter efficiently inhibited AP-mediated cell lysis (Fig. 2B). However, inhibition of FD *in vivo* presents the challenge of overcoming the high resynthesis rates of approximately 1.33 mg/kg/day in humans (46).

In an AP-mediated *in vitro* model of C3 glomerulopathy, inhibition of FB failed to provide complete protection against C3 deposition on endothelial cells (Fig. 4B). Consistent with previous reports, inhibition of C5 resulted in marked residual lytic activities despite a comfortable surplus of the C5 inhibitors over the C5 concentration in the assay (e.g. Fig. 2C) (17, 18, 47, 48). C3 inhibition within a CP setting failed to protect from lysis (Fig. 3B), which is also consistent with previous *in vitro* and *in vivo* data and suggests C3-bypass activation of C5 (19, 21, 26). As a convertase-directed inhibitor, TriFu does not appear to exhibit residual C3-opsonisation and/or residual TP activities as is the case with stoichiometric inhibitors. The different mode of inhibition of TriFu, which is more of a regulator than an inhibitor, is also reflected in the flatter inhibition curves, in contrast to the inhibition curves of stoichiometric inhibitors, which typically have steeper slopes (Figs. 2C and 3, B and C, 4B).

In a bactericidal serum test, TriFu was compared to C3, FB, and C5 inhibitors. For this purpose, all inhibitors were used at individual final concentrations that had showed a “plateau effect” in protecting vulnerable erythrocytes. While the AP-selective inhibitors of FB and C3 did not affect complement-mediated bactericidal activity in serum, C5 inhibition and inhibition of all three complement activation pathways by TriFu noticeably affected the ability of serum to lyse *E. coli* cells *in vitro* (Fig. 5). It is reasonable to assume that inhibition of all pathways by TriFu or by a C5-inhibitor that blocks the common TP will more severely impair the bactericidal activities of complement. Blocking C5 activation in the *E. coli* lysis assay still allowed for considerable clearance of bacteria through MAC formation, presumably due to residual C5 activity mentioned previously (43). TriFu impaired serum bactericidal activity to a comparable extent as C5 inhibition did. Although TriFu will not stop the deposition of C4b opsonins, it efficiently interferes with C3b deposition. Therefore, it will be important to investigate the effects of TriFu on bacterial infections *in vivo* in future studies. A remarkable observation is that by combining much lower concentrations of TriFu (that are not yet sufficient to stop complement activity on its own) with large amounts of C5 inhibitors (which due to the intrinsic residual lytic activity of C5 in presence of C5 inhibitor are unable to stop lysis) a complete protection against complement-mediated cell lysis can be achieved (Fig. 3D). This can be interpreted as a synergy between TriFu and C5 inhibitors. Suboptimal amounts of TriFu are sufficient to tame the strong complement activation response to

such an extent that the remaining residual C5 activity in presence of C5 inhibitors is abolished. This is because TriFu limits the density of the C3b molecules that are deposited onto the cell surface (18, 19).

Given the highly efficient and completely protective activity toward all three complement initiation pathways (Fig. 6), TriFu is warranted to be investigated in upcoming *in vivo* studies of complement-mediated diseases with a strong or broad activation profile. Its broad complement regulating profile toward all pathways, its targeting functionality toward late stage C3 opsonins (iC3b and C3dg) and host surface marker (glycosaminoglycans and sialic acids), and its nonstoichiometric mode of action underline the unique opportunity of this regulator to potentially address complement pathophysiology that is driven by very strong activation of all three complement initiation pathways.

### Experimental procedures

#### Protein expression and purification

Genes encoding the desired amino acid sequences were purchased from Genent (Thermo Fisher Scientific) and cloned into the pPICZαB expression vector (Invitrogen). TriFu and CR1(15–17) variants were recombinantly expressed in *P. pastoris* KM71H using a lab-scale fermenter with small modifications as previously published (32, 34). Protein purification was accomplished by ion exchange and size exclusion chromatography, similarly to that described previously (32, 34, 49). In most cases, the N-glycosylation sites were removed by mutating the consensus asparagine to a glutamine residue. For constructs with consensus N-glycosylation sites still present, the endoglycosidase H (Endo Hf, new England Biolabs) was used to deglycosylate the proteins, as described before (34). Purity and identity of the purified proteins were confirmed by SDS-PAGE analysis similarly as reported before (32). Aliquots of the engineered complement regulators in PBS were shock frozen in liquid nitrogen and stored at –80 °C until analysis.

#### Complement inhibitors

Ecuzumab and ravulizumab were obtained from remnants in infusion lines. CP40, a peptide of the compstatin family which binds C3 and inhibits its activation by convertases, was a kind gift of Dr Lambris, University of Pennsylvania, Philadelphia, USA (10, 50). MiniFH, sCR1, OmCI, and PAS-OmCI were produced or obtained as previously described (32, 51, 52). The following inhibitors or surrogates of inhibitors in clinical development were produced externally with the help of commercial vendors: anti-C5 mAb (anti-C5), anti-Factor D mAb (anti-FD), C3-inhibitor (APL-2), and FB inhibitor (LNP023).

#### Blood components

Human serum was obtained commercially or gained from healthy donors. In the latter case, it was collected in VACUETTE/S-Monovette serum collection tubes. Aliquots were frozen in liquid nitrogen and were stored at –80 °C. Standardized normal human serum (NHS) and FH-depleted serum were obtained from CompTech. Blood samples from patients with PNH were

## Complete complement inhibition by enzyme-like fusion protein

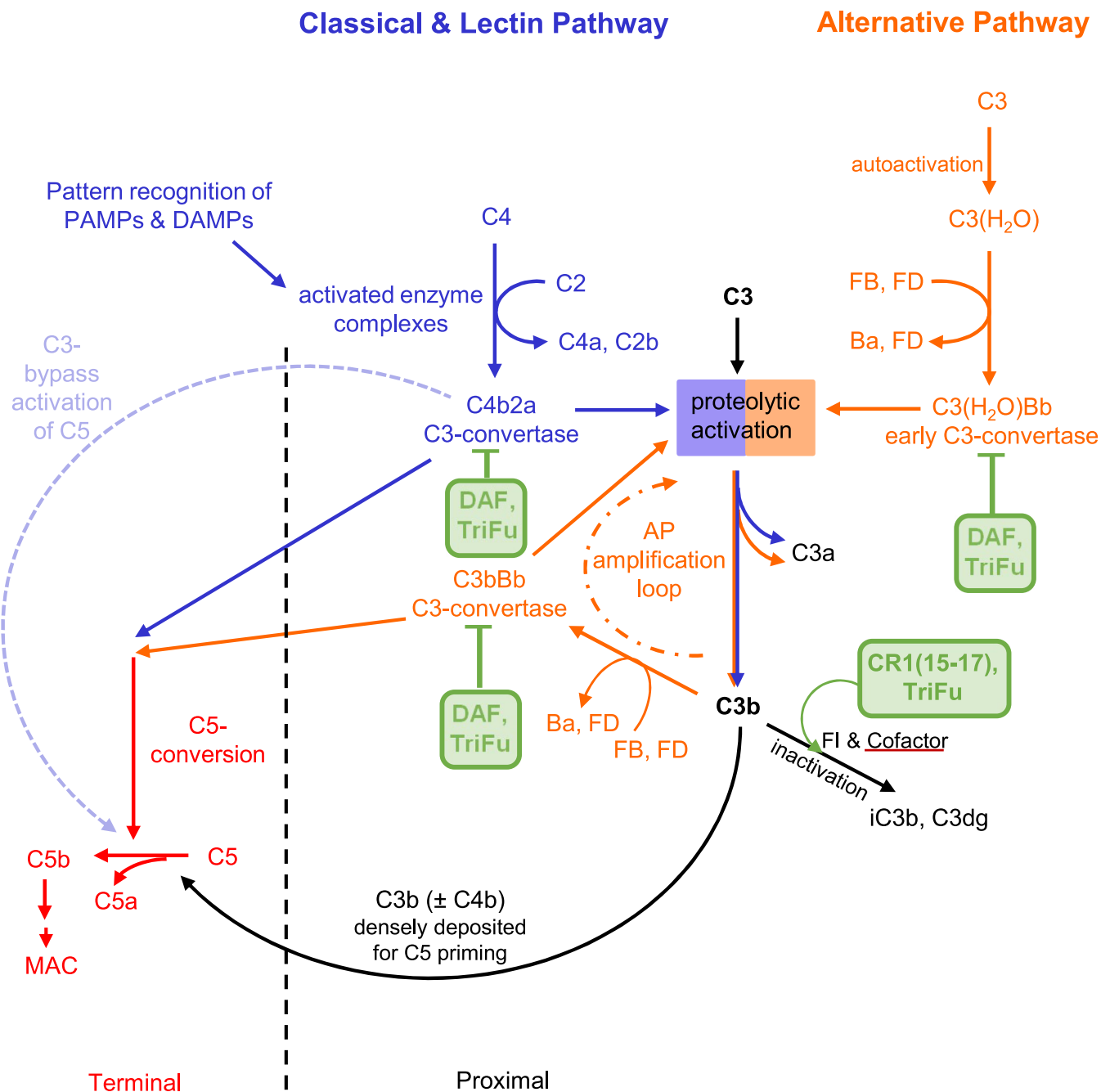


**Figure 6. Schematic illustration of the complement cascade and targets of TriFu and its building blocks with complement regulatory function.** The complement cascade was adapted from Mannes *et al.* 2021 and Schmidt *et al.* 2016. TriFu has decay accelerating activity toward all pathways as the natural regulator DAF. TriFu also has cofactor activity toward all pathways targeting C4b and C3b as the natural regulator CR1 (for simplicity only C3b cofactor activity is shown). Decay acceleration and cofactor activity of TriFu combined with the targeting functionality of Factor H (not shown) results in an efficient inhibitor of all three complement activation pathways: TriFu targets the activated complement proteins of the classical/lectin and alternative pathway that assemble the convertases (C4b, C3b, C4b, C3bBb, and C4b2a) while it does not affect the constitutively expressed precursors (C2, C3, C4, and Factor B). CR1, complement receptor 1; DAF, decay accelerating factor; TriFu, triple fusion complement inhibitor.

collected in EDTA collection tubes by venepuncture and the erythrocytes were used for the PNH hemolysis assays. Blood was taken with approval of the institutional Ethics Committee at Ulm University. All participating volunteers provided written informed consent to participate in this study. The studies abide by the Declaration of Helsinki principles.

Sheep and rabbit erythrocytes in Alsever's solution were purchased from Fiebig Nährstofftechnik GbR.

### Cell culture

HMEC-1 were obtained from the American Type Culture Collection. Cells were cultured according to the suppliers' recommendations. Briefly, the cells were grown in MCDB 131 medium (Life Technologies) containing 10% fetal calf serum (Life Technologies), 2 mM glutamine (Biochrom), 100 U/ml penicillin and 100 µg/ml streptomycin (Life Technologies). Subsequently, 1 µg/ml hydrocortisone (Rotexmedica) and 10 ng/ml epidermal

growth factor (Sigma-Aldrich) were added to the medium shortly before cultivation of the cells at 37 °C and 5% CO<sub>2</sub>.

### Alternative pathway rabbit erythrocyte hemolysis assay

The hemolysis assay was performed as previously described (18, 19, 43). Rabbit erythrocytes were washed with PBS. Serum from healthy donors or NHS (CompTech) was supplemented with 5 mM Mg-EGTA to inhibit any CP activation. Serum was mixed with analytes diluted in PBS or a control (PBS/EDTA, 5 mM or 10 mM). Rabbit erythrocytes were added in the last step (final assay volume was 100 µl). Samples were incubated for 20 or 30 min (depending on the assay) at 37 °C under shaking conditions. After incubation, the reactions were stopped with PBS that had been supplemented with EDTA (to 50 mM or 5 mM depending on the assay). Absorbance of the supernatant was measured at 405 nm. Hemolysis was quantified after blank subtraction (containing the respective serum concentration). Total lysis in water served as a 100% lysis reference control.

### Classical pathway sheep erythrocyte hemolysis assay

CP-mediated hemolysis assays were performed as published (19). Sheep erythrocytes were washed with PBS supplemented with 5 mM EDTA (PBSE). In the next step, sheep erythrocytes were sensitized with rabbit anti-sheep hemolysin (Rockland antibodies & assays) for 20 min at 37 °C. To catch possible naturally occurring antibodies against Forssman antigens in the used sera, the sera were preincubated with equal amounts of washed and packed sheep erythrocytes. This step ensures that the CP is activated exclusively by rabbit anti-sheep hemolysin. Sheep erythrocytes were resuspended in PBS supplemented with 0.15 mM CaCl<sub>2</sub> and 0.5 mM MgCl<sub>2</sub> (PBS<sup>++</sup>). Serial dilutions of analytes were prepared in PBS. Respective controls consisted of PBS, EDTA, or EGTA at a final assay concentration of 5 or 10 mM. Inhibitors and control compounds were mixed with the respective amount of preadsorbed serum. Sheep erythrocytes suspended in PBS<sup>++</sup> were added in the last step. The prepared mixtures were incubated for 1 h at 37 °C under shaking conditions. Reactions were stopped by adding 50 µl of ice-cold PBSE. Hemolysis was quantified by measuring the absorbance of the supernatant at 405 nm. Respective blank solutions containing the same serum amount as the mixtures in the assay were subtracted. Total lysis in water served as a reference control for 100% lysis.

### PNH erythrocyte hemolysis assay

The PNH hemolysis assay follows the principle of Ham's test and was performed with small modifications as published before (43, 53).

Briefly, PNH erythrocytes were washed with PBS. Either the serum from donors with blood group AB was supplemented with MgCl<sub>2</sub> (to reach final Mg-ion concentration in the assay of 1.5 mM) or the serum from healthy volunteers (without blood group typing) was supplemented with 1.5 mM MgCl<sub>2</sub> and 5 mM EGTA to ensure that lysis is mediated only by the AP.

The serum was acidified (pH 6.6–6.9) using 1 M HCl triggering brisk AP activation (54). Then, 30 µl of the acidified serum were mixed with 8 µl of an inhibitor solution or PBS and incubated on ice for 5 min. Two microliters of packed PNH erythrocytes were added. Then the reactions were incubated in 0.2 ml tubes at 37 °C for 24 h while shaking at 1200 rpm. To analyze the level of hemolysis in the supernatant, cells were spun down, and absorbance was measured at 405 nm. Total lysis in water served as a 100% lysis reference control.

### Classical pathway PNH erythrocyte hemolysis assay

In an assay adapted from Harder *et al.* (18), PNH erythrocytes were sensitized with an alloantibody. After washing in PBSE, the PNH erythrocytes were incubated for 20 min at 37 °C under shaking conditions. The source of the alloantibody was an anti-PP1Pk citrate plasma that had been diluted with PBSE (1:10). After incubation, cells were washed again with PBSE and then with PBS<sup>++</sup>. The alloantibody sensitized erythrocytes were resuspended in PBS<sup>++</sup>. Human serum at a concentration of 50% was supplemented with the respective inhibitors or controls. As controls served reaction with PBS or 10 mM EDTA or 10 mM EGTA. In the end, 10 µl of the erythrocyte suspension was added. The final assay volume was 100 µl. The samples were incubated for 90 min at 37 °C under shaking conditions. The reaction was stopped by adding a PBS-EDTA solution (containing EDTA at 50 mM, 50 µl). Hemolysis was quantified by measuring the absorbance of the supernatant at 405 nm. In addition to measuring released hemoglobin using spectrophotometry, flow cytometry was used in representative assays to verify that the complement sensitive PNH III erythrocytes, which lack CD59, have lysed (in contrast to the protected PNH I erythrocytes). A R-phycoerythrin-labeled mAb against human CD59 (clone: OV9A2, Isotype: IgG1κ, Affymetrix eBioscience) was used.

### Endothelial C3b-opsonization assay

The HMEC-1 assay was performed as previously described (55). HMEC-1 cells were seeded in 24-well plates (50.000 cells/well). One day later fresh medium was added. The next day, medium was removed, and a 40% solution of commercially available factor H-depleted serum (±5 mM EGTA) diluted in PBS was added. This serum dilution was supplemented with different concentrations of the analytes. The final volume of the serum mix added to the culture plate was 300 µl. To activate the complement cascade 1 mM MgCl<sub>2</sub> was supplemented as last step. Cells were incubated for 1 h at 37 °C. Heat-inactivated serum and NHS served as controls. After incubation, the cells were detached with trypsin/EDTA and incubated with a biotinylated anti-human C3d antibody (A702 from Quidel) (1:100 in PBS) for 10 min at room temperature. Cells were washed with PBS followed by incubation with allophycocyanin-conjugated streptavidin (SA1005, Invitrogen) (1:100 in PBS) for 30 min at room temperature. Cells were washed again with PBS, and C3d opsonization was analyzed by flow cytometry (BD FACSVerser).

## Complete complement inhibition by enzyme-like fusion protein

### Surface plasmon resonance

Experiments were performed on a Reichert SR7500DC SPR instrument at 25 °C. For binding analysis of the engineered complement regulators, carboxymethyl dextran (CMD500) sensor chips (Xantec Bioanalytics) were used. C3b, iC3b, C3d, and C4b (CompTech) were immobilized *via* standard amine coupling. Binding to C4b was also analyzed when C4b was captured in a more physiological orientation. For this purpose, C4b was biotinylated at the free sulfhydryl group of the thio-ester moiety and was fixed on a sensor chip surface coated with avidin as described before (SAP from Xantec Bioanalytics) (19). Dilution series (1:1) of the engineered proteins were prepared in SPR running buffer (0.005% Tween 20 in PBS or Hepes buffered saline containing 1 mM MgCl<sub>2</sub>). The analytes were injected for 2 to 3 min at a flow rate of 25 μl/min, followed by flow of SPR running buffer for 5 min. To regenerate the chip surface 1 M NaCl was injected for 0.5 or 1 min, followed by a flow of SPR running buffer. Only reference subtracted sensorgrams are shown. Equilibrium dissociation constants ( $K_D$ ) were determined by plotting binding response against the analyte concentrations and applying a 1:1 steady-state affinity model using TraceDrawer (<https://tracedrawer.com/>) software.

In addition, a Biacore 8K SPR instrument was used at an assay temperature of 25 °C and a flow rate of 30 μl/min. Running buffer was Hepes buffered saline-EP+ containing 10 mM Hepes, 150 mM NaCl, 3 mM EDTA, 0.05% (v/v) Tween 20, and 1 mM MgCl<sub>2</sub> at pH 7.4. The sensor chips used were series S sensor chips (CM5 from GE HealthCare). C3b was amine-coupled onto the CM5 chip using standard amine coupling. 1:1 dilution series of binding partners were injected onto the surface to measure the respective binding curves and affinities, were appropriate. Regeneration was achieved by applying running buffer until complete analyte dissociation occurred. To determine apparent equilibrium dissociation constants ( $K_D$ ), all data were double-referenced prior to fitting them to a steady-state affinity model using the Biacore Insight Evaluation (<https://www.cytivalifesciences.com/en/us/shop/protein-analysis/spr-label-free-analysis/spr-software-and-extensions/biacore-insight-evaluation-software-p-23528>) Software v3.0 (GE HealthCare).

### E. coli survival assay

A total of 10 ml of LB medium containing the antibiotic Zeocin (at a final concentration of 25 μg/ml) were inoculated with 500 μl (1:20 dilution) of an overnight starter culture of the *E. coli* strain XL1-blue (Agilent Technologies), which had previously been transformed with the pPICZαB plasmid (Thermo Fisher Scientific). The culture was grown (at 37 °C while shaking) until an OD<sub>600</sub> of 0.6 was reached. Then the pellet was harvested and resuspended in PBS (10 ml). Twenty-five microliters of serum (NHS or heat-inactivated serum) were mixed with 5 μl PBS (control) or compound (diluted in PBS) and 20 μl of the *E. coli*-PBS suspension. This mixture was incubated on ice for 30 min. The final content of serum was 50%. Then samples were incubated at 37 °C while shaking at

100 rpm for 1 h. Afterward the samples were placed on ice and kept on ice for 1 h. Each sample was diluted 1:1000 and 1:10,000, 1:100,000, 1:1,000,000 in PBS. Subsequently, 100 μl of each dilution was spread onto fresh LB-Zeocin-agar plates and incubated overnight at 37 °C. The serial dilutions were achieved by mixing 15 μl of sample with 135 μl of PBS. Colonies were counted for each plate.

### Statistical methods

If not indicated otherwise data are presented as mean ± SD. IC<sub>50</sub> values of inhibitors were calculated using GraphPad Prism (<https://www.graphpad.com/features>) software and a sigmoidal fit of the dose-response curves. The goodness of fit is indicated by R<sup>2</sup>.

### Data availability

The data that support the findings of this study are included in the main article and Supplementary Information file.

---

*Supporting information*—This article contains supporting information (27–29, 31, 32).

*Author contributions*—S. J. S., A. D., K. K., B. K. G., M. M., A. A., M. A., and N. S. investigation; S. J. S., A. D., K. K., B. K. G., M. M., A. A., M. A., and N. S. formal analysis; S. J. S., A. D., K. K., B. K. G., M. M., N. S., A. A., B. H., H. S., M. A., R. B., M. H.-L., and C. Q. S. writing—review and editing; S. J. S., A. D., K. K., B. K. G., M. M., B. H., H. S., and R. B. resources; S. J. S., A. D., K. K., B. K. G., M. M., B. H., H. S., and R. B. methodology; B. H., H. S., R. B., M. H.-L., and C. Q. S. supervision; B. H., H. S., R. B., M. H.-L., and C. Q. S. data curation; B. H., H. S., R. B., M. A., M. H.-L., and C. Q. S. conceptualization.

*Funding and additional information*—This work was supported by Deutsche Forschungsgemeinschaft grants SCHM 3018/4-1 (to C. Q. S.) and funding by Takeda Pharmaceuticals.

*Conflict of interest*—C. Q. S., H. S., B. H., A. D. and M. H.-L. are inventors of (a) patent application(s) that describes the use of complement inhibitors for therapeutic applications. C. Q. S. has received research funding from pharmaceutical companies. M. H.-L., C. Q. S., B. H. and H. S. received honoraria for speaking at symposia organized by Alexion Pharmaceuticals. H. S. served on advisory committees for Alexion AstraZeneca Rare Diseases, Sanofi, Sobi, Novartis, Amgen and received research funding from Alexion Pharmaceuticals (all to the University of Ulm). The other authors have disclosed no relevant conflict of interest with the contents of the article. B. K. G. and R. B. were/are employees at Takeda Pharmaceuticals.

*Abbreviations*—The abbreviations used are: anti-FD, anti-factor D; AP, alternative pathway; CA, cofactor activity; CP/LP, classical/lectin pathway; CR1, complement receptor 1; DAA, decay accelerating activity; DAF, decay accelerating factor; FB, factor B; FH, factor H; HMEC, human microvascular endothelial cells; LL, long linker; MAC, membrane attack complex; NHS, normal human serum; OmCI, *Ornithodoros moubata* complement inhibitor; PAS-OmCI, PASylated version of OmCI; PBSE, PBS supplemented with 5 mM EDTA; PNH, paroxysmal nocturnal hemoglobinuria; sCR1,

soluble complement receptor 1; SL, short linker; SPR, surface plasmon resonance; TP, terminal pathway; TriFu, triple fusion complement inhibitor.

## References

- Hillmen, P., Young, N. S., Schubert, J., Brodsky, R. A., Socié, G., Muus, P., *et al.* (2006) The complement inhibitor eculizumab in paroxysmal nocturnal hemoglobinuria. *N. Engl. J. Med.* **355**, 1233–1243
- Legendre, C. M., Licht, C., Muus, P., Greenbaum, L. A., Babu, S., Bedrosian, C., *et al.* (2013) Terminal complement inhibitor eculizumab in atypical hemolytic-uremic syndrome. *N. Engl. J. Med.* **368**, 2169–2181
- Howard, J. F., Utsugisawa, K., Benatar, M., Murai, H., Barohn, R. J., Illa, I., *et al.* (2017) Safety and efficacy of eculizumab in anti-acetylcholine receptor antibody-positive refractory generalised myasthenia gravis (REGAIN): a phase 3, randomised, double-blind, placebo-controlled, multicentre study. *Lancet Neurol.* **16**, 976–986
- Pitcock, S. J., Berthele, A., Fujihara, K., Kim, H. J., Levy, M., Palace, J., *et al.* (2019) Eculizumab in aquaporin-4-positive neuromyelitis optica spectrum disorder. *N. Engl. J. Med.* **381**, 614–625
- Lee, J. W., Sicre de Fontbrune, F., Wong Lee Lee, L., Pessoa, V., Gualandro, S., Füreder, W., *et al.* (2019) Ravulizumab (ALXN1210) vs eculizumab in adult patients with PNH naive to complement inhibitors: the 301 study. *Blood* **133**, 530–539
- Kulasekararaj, A. G., Hill, A., Rottinghaus, S. T., Langemeijer, S., Wells, R., Gonzalez-Fernandez, F. A., *et al.* (2019) Ravulizumab (ALXN1210) vs eculizumab in C5-inhibitor-experienced adult patients with PNH: the 302 study. *Blood* **133**, 540–549
- Rother, R. P., Rollins, S. A., Mojcik, C. F., Brodsky, R. A., and Bell, L. (2007) Discovery and development of the complement inhibitor eculizumab for the treatment of paroxysmal nocturnal hemoglobinuria. *Nat. Biotechnol.* **25**, 1256–1264
- Sheridan, D., Yu, Z.-X., Zhang, Y., Patel, R., Sun, F., Lasaro, M. A., *et al.* (2018) Design and preclinical characterization of ALXN1210: a novel anti-C5 antibody with extended duration of action. *PLoS One* **13**, e0195909
- Hillmen, P., Szer, J., Weitz, I., Röth, A., Höchsmann, B., Panse, J., *et al.* (2021) Pegcetacoplan versus eculizumab in paroxysmal nocturnal hemoglobinuria. *N. Engl. J. Med.* **384**, 1028–1037
- Lamers, C., Mastellos, D. C., Ricklin, D., and Lambris, J. D. (2022) Compstatins: the dawn of clinical C3-targeted complement inhibition. *Trends Pharmacol. Sci.* **43**, 629–640
- Janssen, B. J. C., Half, E. F., Lambris, J. D., and Gros, P. (2007) Structure of compstatin in complex with complement component C3c reveals a new mechanism of complement inhibition. *J. Biol. Chem.* **282**, 29241–29247
- Risitano, A. M., Notaro, R., Marando, L., Serio, B., Ranaldi, D., Seneca, E., *et al.* (2009) Complement fraction 3 binding on erythrocytes as additional mechanism of disease in paroxysmal nocturnal hemoglobinuria patients treated by eculizumab. *Blood* **113**, 4094–4100
- Hill, A., Rother, R. P., Arnold, L., Kelly, R., Cullen, M. J., Richards, S. J., *et al.* (2010) Eculizumab prevents intravascular hemolysis in patients with paroxysmal nocturnal hemoglobinuria and unmasks low-level extravascular hemolysis occurring through C3 opsonization. *Haematologica* **95**, 567–573
- Höchsmann, B., Leichtle, R., von Zabern, I., Kaiser, S., Flegel, W. A., and Schrezenmeier, H. (2012) Paroxysmal nocturnal haemoglobinuria treatment with eculizumab is associated with a positive direct antiglobulin test. *Vox Sang.* **102**, 159–166
- Risitano, A. M. (2015) Dissecting complement blockade for clinic use. *Blood* **125**, 742–744
- Risitano, A. M., and Marotta, S. (2018) Toward complement inhibition 2.0: next generation anticomplement agents for paroxysmal nocturnal hemoglobinuria. *Am. J. Hematol.* **93**, 564–577
- Harder, M. J., Höchsmann, B., Dopler, A., Anliker, M., Weinstock, C., Skerra, A., *et al.* (2019) Different levels of incomplete terminal pathway inhibition by eculizumab and the clinical response of PNH patients. *Front. Immunol.* **10**, 1639
- Harder, M. J., Kuhn, N., Schrezenmeier, H., Höchsmann, B., von Zabern, I., Weinstock, C., *et al.* (2017) Incomplete inhibition by eculizumab: mechanistic evidence for residual C5 activity during strong complement activation. *Blood* **129**, 970–980
- Mannes, M., Dopler, A., Zolk, O., Lang, S. J., Halbgebauer, R., Höchsmann, B., *et al.* (2021) Complement inhibition at the level of C3 or C5: mechanistic reasons for ongoing terminal pathway activity. *Blood* **137**, 443–455
- Schrezenmeier, H., Kulasekararaj, A., Mitchell, L., Sicre de Fontbrune, F., Devos, T., Okamoto, S., *et al.* (2020) One-year efficacy and safety of ravulizumab in adults with paroxysmal nocturnal hemoglobinuria naive to complement inhibitor therapy: open-label extension of a randomized study. *Ther. Adv. Hematol.* **11**, 2040620720966137
- Zhang, L., Dai, Y., Huang, P., Saunders, T. L., Fox, D. A., Xu, J., *et al.* (2019) Absence of complement component 3 does not prevent classical pathway-mediated hemolysis. *Blood Adv.* **3**, 1808–1814
- Schmitz, R., Fitch, Z. W., Schroder, P. M., Choi, A. Y., Manook, M., Yoon, J., *et al.* (2021) C3 complement inhibition prevents antibody-mediated rejection and prolongs renal allograft survival in sensitized non-human primates. *Nat. Commun.* **12**, 5456
- Baas, I., Delvasto-Nuñez, L., Ligthart, P., Brouwer, C., Folman, C., Reis, E. S., *et al.* (2020) Complement C3 inhibition by compstatin Cp40 prevents intra- and extravascular hemolysis of red blood cells. *Haematologica* **105**, e57–e60
- Fiane, A. E., Mollnes, T. E., Videm, V., Hovig, T., Høgåsen, K., Mellbye, O. J., *et al.* (1999) Compstatin, a peptide inhibitor of C3, prolongs survival of ex vivo perfused pig xenografts. *Xenotransplantation* **6**, 52–65
- Abicht, J.-M., Kourtzelis, I., Reichart, B., Koutsogiannaki, S., Primikyri, A., Lambris, J. D., *et al.* (2017) Complement C3 inhibitor Cp40 attenuates xenoreactions in pig hearts perfused with human blood. *Xenotransplantation* **24**. <https://doi.org/10.1111/xen.12262>
- Skendros, P., Germainidis, G., Mastellos, D. C., Anantiadou, C., Gavriilidis, E., Kalopitas, G., *et al.* (2022) Complement C3 inhibition in severe COVID-19 using compstatin AMY-101. *Sci. Adv.* **8**, eabo2341
- Kuttner-Kondo, L., Hourcade, D. E., Anderson, V. E., Muqim, N., Mitchell, L., Soares, D. C., *et al.* (2007) Structure-based mapping of DAF active site residues that accelerate the decay of C3 convertases. *J. Biol. Chem.* **282**, 18552–18562
- Fornieris, F., Wu, J., Xue, X., Ricklin, D., Lin, Z., Sfyroera, G., *et al.* (2016) Regulators of complement activity mediate inhibitory mechanisms through a common C3b-binding mode. *EMBO J.* **35**, 1133–1149
- Krych, M., Clemenza, L., Howdeshell, D., Hauhart, R., Hourcade, D., and Atkinson, J. P. (1994) Analysis of the functional domains of complement receptor type 1 (C3b/C4b receptor; CD35) by substitution mutagenesis. *J. Biol. Chem.* **269**, 13273–13278
- Krych, M., Hauhart, R., and Atkinson, J. P. (1998) Structure-function analysis of the active sites of complement receptor type 1. *J. Biol. Chem.* **273**, 8623–8629
- Brodbeck, W. G., Liu, D., Sperry, J., Mold, C., and Medof, M. E. (1996) Localization of classical and alternative pathway regulatory activity within the decay-accelerating factor. *J. Immunol.* **156**, 2528–2533
- Schmidt, C. Q., Bai, H., Lin, Z., Risitano, A. M., Barlow, P. N., Ricklin, D., *et al.* (2013) Rational engineering of a minimized immune inhibitor with unique triple-targeting properties. *J. Immunol.* **190**, 5712–5721
- Xue, X., Wu, J., Ricklin, D., Fornieris, F., Di Crescenzo, P., Schmidt, C. Q., *et al.* (2017) Regulator-dependent mechanisms of C3b processing by factor I allow differentiation of immune responses. *Nat. Struct. Mol. Biol.* **24**, 643–651
- Schmidt, C. Q., Slingsby, F. C., Richards, A., and Barlow, P. N. (2011) Production of biologically active complement factor H in therapeutically useful quantities. *Protein Expr. Purif.* **76**, 254–263
- Schmidt, C. Q., Herbert, A. P., Kavanagh, D., Gandy, C., Fenton, C. J., Blaum, B. S., *et al.* (2008) A new map of glycosaminoglycan and C3b binding sites on factor H. *J. Immunol.* **181**, 2610–2619

## Complete complement inhibition by enzyme-like fusion protein

36. Schmidt, C. Q., Lambris, J. D., and Ricklin, D. (2016) Protection of host cells by complement regulators. *Immunol. Rev.* **274**, 152–171
37. Tetteh-Quarcoo, P. B., Schmidt, C. Q., Tham, W.-H., Hauhart, R., Mertens, H. D. T., Rowe, A., *et al.* (2012) Lack of evidence from studies of soluble protein fragments that Knops blood group polymorphisms in complement receptor-type 1 are driven by malaria. *PLoS One* **7**, e34820
38. Morgan, H. P., Schmidt, C. Q., Guariento, M., Blaum, B. S., Gillespie, D., Herbert, A. P., *et al.* (2011) Structural basis for engagement by complement factor H of C3b on a self surface. *Nat. Struct. Mol. Biol.* **18**, 463–470
39. Harris, C. L., Abbott, R. J. M., Smith, R. A., Morgan, B. P., and Lea, S. M. (2005) Molecular dissection of interactions between components of the alternative pathway of complement and decay accelerating factor (CD55). *J. Biol. Chem.* **280**, 2569–2578
40. Harris, C. L., Pettigrew, D. M., Lea, S. M., and Morgan, B. P. (2007) Decay-accelerating factor must bind both components of the complement alternative pathway C3 convertase to mediate efficient decay. *J. Immunol.* **178**, 352–359
41. Konar, M., and Granoff, D. M. (2017) Eculizumab treatment and impaired opsonophagocytic killing of meningococci by whole blood from immunized adults. *Blood* **130**, 891–899
42. Ispasanie, E., Muri, L., Schubart, A., Thorburn, C., Zamurovic, N., Holbro, T., *et al.* (2021) Alternative complement pathway inhibition does not Abrogate Meningococcal killing by serum of vaccinated individuals. *Front. Immunol.* **12**, 747594
43. Schmidt, C. Q., Harder, M. J., Nichols, E.-M., Hebecker, M., Anliker, M., Höchsmann, B., *et al.* (2016) Selectivity of C3-opsonin targeted complement inhibitors: a distinct advantage in the protection of erythrocytes from paroxysmal nocturnal hemoglobinuria patients. *Immunobiology* **221**, 503–511
44. Wang, C.-Y., Wang, S.-W., Huang, W.-C., Kim, K. S., Chang, N.-S., Wang, Y.-H., *et al.* (2012) Prc contributes to Escherichia coli evasion of classical complement-mediated serum killing. *Infect. Immun.* **80**, 3399–3409
45. Schmidt, C. Q., and Smith, R. J. H. (2023) Protein therapeutics and their lessons: expect the unexpected when inhibiting the multi-protein cascade of the complement system. *Immunol. Rev.* **313**, 376–401
46. Pascual, M., Steiger, G., Estreicher, J., Macon, K., Volanakis, J. E., and Schifferli, J. A. (1988) Metabolism of complement factor D in renal failure. *Kidney Int.* **34**, 529–536
47. Wehling, C., Amon, O., Bommer, M., Hoppe, B., Kentouche, K., Schalk, G., *et al.* (2017) Monitoring of complement activation biomarkers and eculizumab in complement-mediated renal disorders. *Clin. Exp. Immunol.* **187**, 304–315
48. Gupta, S., Fenves, A., Nance, S. T., Sykes, D. B., and Dzik, W. S. (2015) Hyperhemolysis syndrome in a patient without a hemoglobinopathy, unresponsive to treatment with eculizumab. *Transfusion* **55**, 623–628
49. Schmidt, C. Q., Herbert, A. P., Mertens, H. D. T., Guariento, M., Soares, D. C., Uhrin, D., *et al.* (2010) The central portion of factor H (modules 10–15) is compact and contains a structurally deviant CCP module. *J. Mol. Biol.* **395**, 105–122
50. Mastellos, D. C., Yancopoulou, D., Kokkinos, P., Huber-Lang, M., Hajishengallis, G., Biglarnia, A. R., *et al.* (2015) Compstatin: a C3-targeted complement inhibitor reaching its prime for bedside intervention. *Eur. J. Clin. Invest.* **45**, 423–440
51. Tham, W.-H., Schmidt, C. Q., Hauhart, R. E., Guariento, M., Tetteh-Quarcoo, P. B., Lopaticki, S., *et al.* (2011) Plasmodium falciparum uses a key functional site in complement receptor type-1 for invasion of human erythrocytes. *Blood* **118**, 1923–1933
52. Kuhn, N., Schmidt, C. Q., Schlapschy, M., and Skerra, A. (2016) PASylated coversin, a C5-specific complement inhibitor with extended pharmacokinetics, shows enhanced anti-hemolytic activity *in Vitro*. *Bioconjug. Chem.* **27**, 2359–2371
53. Ham, T. H. (1937) Chronic hemolytic anemia with paroxysmal nocturnal hemoglobinuria: study of the mechanism of hemolysis in relation to acid-base equilibrium. *N. Engl. J. Med.* **217**, 915–917
54. Wilcox, L. A., Ezzell, J. L., Bernshaw, N. J., and Parker, C. J. (1991) Molecular basis of the enhanced susceptibility of the erythrocytes of paroxysmal nocturnal hemoglobinuria to hemolysis in acidified serum. *Blood* **78**, 820–829
55. Dopler, A., Guntau, L., Harder, M. J., Palmer, A., Höchsmann, B., Schrezenmeier, H., *et al.* (2019) Self versus Nonself Discrimination by the soluble complement regulators factor H and FHL-1. *J. Immunol.* **202**, 2082–2094